A DFIG Sensorless Rotor-Position Detector Based on a Hysteresis Controller

G. D. Marques, *Member, IEEE*, V. Fernão Pires, *Senior Member, IEEE*, Sérgio Sousa, and Duarte M. Sousa, *Member, IEEE*

***Abstract*—A simple sensorless method for the detection of the mechanical rotor position of the wound-rotor induction machine in order to implement stator-flux orientation is described and evaluated in this paper. The method is based on the phase comparison of the actual and the estimated rotor currents using the classical model of the machine. It can be conceptually implemented in the rotor or in the stator reference frames. It has some similarity to the model reference adaptive system methodology, but uses a hysteresis comparator instead of a proportional integral (PI) controller. In this way, the method does not need parameter determination for the controllers and shows a considerable independence of parameter uncertainties. Simulation and experimental results show that the method is appropriate for the vector control of the doubly fed induction generator (DFIG) because it leads to the decoupling of active and reactive power chains. It is also appropriate for the control of the DFIG in transients like those when voltage dips occur.**

***Index Terms*—Doubly fed induction generators (DFIGs), induction generators, sensorless.**

NOMENCLATURE

General

E	Estimated.
i	Stator or rotor current.
k_f	Parameter for initial conditions effects.
k_p, T_i	Parameters of the PI controller.
L_s	Stator inductance.
M	Measured.
M	Mutual inductance.
P_e	Active power transferred to the rotor.
Q_s	Reactive power.
r_s	Stator resistance.
T_s	Sampling time.
u	Stator voltage.
ε_r	Error.
γ_s	Position of the stator-flux vector.
γ_m	Electrical position of the rotor.
ω_s	Electrical frequency of the ac mains.
ω_c	Crossover frequency.
ψ	Stator or rotor flux linkage.

Superscripts

$\hat{}$	Estimated value.
s, r	Stator or rotor reference frame.

Subscripts

α, β	Usual $\alpha\beta$ variables.
d, q	Variables on a moving reference frame.
s, r	Stator or rotor quantities.

Manuscript received March 5, 2010; revised May 4, 2010 and June 28, 2010; accepted August 18, 2010. Date of publication October 7, 2010; date of current version February 18, 2011. This work was supported in part by the Center for Innovation in Electrical and Energy Engineering, Instituto Superior Técnico, Technical University of Lisbon, and in part by the Programa Operacional da Sociedade do Conhecimento. Paper no. TEC-0086-2010.

G. D. Marques and D. M. Sousa are with the Instituto Superior Técnico, Technical University of Lisbon, Lisbon 1049-001, Portugal (e-mail: gil.marques@ist.utl.pt; duarte.sousa@ist.utl.pt).

V. F. Pires and S. Sousa are with the Department of Electrical Engineering, Superior Technical School of Setúbal, Polytechnic Institute of Setúbal, Setúbal 2910-761, Portugal (e-mail: vitor.pires@estsetubal.ips.pt; sergio.sousa@netvisao.pt).

Digital Object Identifier 10.1109/TEC.2010.2070507

I. INTRODUCTION

THE doubly fed induction generator (DFIG) is very attractive for adjustable speed-constant frequency (ASCF) generators with limited speed range. In this system, the stator circuits of the wound induction machine are directly connected to the ac mains and the rotor circuits are supplied by one back-to-back pulsewidth modulated (PWM) converter. This provides flexibility of operation in subsynchronous and supersynchronous speeds both in the generating and motoring modes. The rating of the power converter is lower than the machine rating and is determined by the operating speed range, normally limited to 1/3 under and above the synchronous speed [1].

The conventional approach for the control of the DFIG is the implementation of stator-field orientation. The performance of the system depends on the detection of the stator-flux reference frame and the detection of the mechanical position of the rotor, derived from a position encoder, as shown in Fig. 1, or from a sensorless detection algorithm, as considered in this paper.

Since the power converter is connected to the rotor, it is mandatory to know the rotor position to implement the proposed control. Although the control is implemented in the field reference frame, it is necessary to use a reference-frame transformation from the field to the rotor reference frame.

There are several position-sensorless methods proposed in [2]–[15]. A preliminary version of the method proposed in this paper, based only on simulations, was published in a conference paper [16].

There are major challenges in designing a position sensorless for a doubly fed wound-rotor induction machine. The algorithm should be stable and work well at any speed of the working range including near the synchronous speed. The rotor-detection-position system should be able to start on the fly, i.e., it should converge to the correct position after some period of time, when the system starts working, without the knowledge of any initial condition [5].

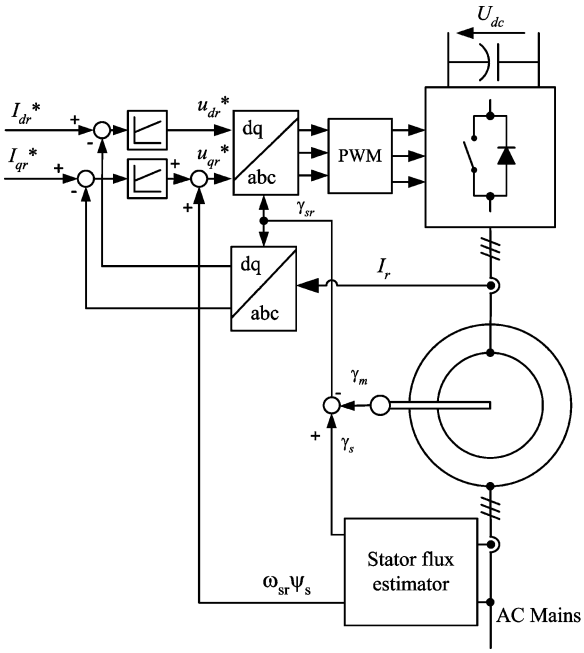

Fig. 1. Block diagram for the implementation of field orientation.

This paper presents a sensorless algorithm to estimate the rotor position that can be implemented in two different reference frames. When the rotor reference frame is adopted, the method proposed here has some similarities to the method proposed in [8]–[10]. When implemented in the stator reference frame, it has some similarities to the phase-locked loop (PLL) method proposed in [14] and [15].

The estimated position determined by this method was compared with the actual position measured using an encoder. The PLL method described in [14] and [15] was also implemented and compared with the method proposed in this paper. To simplify the exposition of the algorithm in this paper and the implementation in the laboratory, *per unit* values are used. When compared with the PLL system, tuned to have a bandwidth as high as 200 Hz, this method presents similar dynamic behavior.

Section II describes the proposed algorithm. Section III presents the stability analysis. Simulation results based on a tool constructed on the MATLAB/Simulink environment are presented in Section IV. Section V presents the synthesis of the PLL method. Section VI presents experimental results obtained with a small prototype constructed for this purpose. Section VII presents the conclusion.

II. Description of the Method

The method proposed in this paper is derived from the classical model of the induction machine. Consider the following voltage equations of the stator circuits on the stator reference frame, in motor convention, and *per unit (p.u.)* values:

$$u_{\alpha s} = r_s i_{\alpha s} + \frac{1}{\omega_s}\frac{d\psi_{\alpha s}}{dt}$$
$$u_{\beta s} = r_s i_{\beta s} + \frac{1}{\omega_s}\frac{d\psi_{\beta s}}{dt}. \quad (1)$$

The stator-flux vector $\boldsymbol{\Psi_s} = (\psi_{as}, \psi_{bs})$ can be obtained using the classic stator-flux estimator based on (1)

$$\psi_{\alpha s} = \omega_s \int (u_{\alpha s} - r_s i_{\alpha s})dt$$
$$\psi_{\beta s} = \omega_s \int (u_{\beta s} - r_s i_{\beta s})dt. \quad (2)$$

Section VI will address the practical implementation of the flux estimator described in (2). Other flux estimators can also be used [17]. The position of the stator-flux angle γ_s, measured in the stator reference frame, is determined by

$$\cos\gamma_s = \frac{\psi_{\alpha s}}{\sqrt{\psi_{\alpha s}^2 + \psi_{\beta s}^2}} \qquad \sin\gamma_s = \frac{\psi_{\beta s}}{\sqrt{\psi_{\alpha s}^2 + \psi_{\beta s}^2}}. \quad (3)$$

The stator-flux vector $\boldsymbol{\Psi_s}$ can also be determined using stator- and rotor-current vectors $\boldsymbol{i_s} = (i_{\alpha s}, i_{\beta s}), \boldsymbol{i_r} = (i_{\alpha r}, i_{\beta r})$ and the rotor-position angle γ_m

$$\psi_{\alpha s} = L_s i_{\alpha s} + M\cos\gamma_m i_{\alpha r} - M\sin\gamma_m i_{\beta r}$$
$$\psi_{\beta s} = L_s i_{\beta s} + M\sin\gamma_m i_{\alpha r} + M\cos\gamma_m i_{\beta r} \quad (4)$$

or

$$\begin{bmatrix}\psi_{\alpha s}\\ \psi_{\beta s}\end{bmatrix} = \begin{bmatrix}L_s i_{\alpha s} + M i_{\alpha r}^s\\ L_s i_{\beta s} + M i_{\beta r}^s\end{bmatrix} \quad (5)$$

where $i_{\alpha s}^s$ and $i_{\beta s}^s$ are the rotor currents in the stator reference frame. These variables are related with the measured rotor currents by

$$\begin{bmatrix}i_{\alpha r}^s\\ i_{\beta r}^s\end{bmatrix} = \begin{bmatrix}\cos\gamma_m & -\sin\gamma_m\\ \sin\gamma_m & \cos\gamma_m\end{bmatrix}\cdot\begin{bmatrix}i_{\alpha r}\\ i_{\beta r}\end{bmatrix}. \quad (6)$$

Equations (5) and (2) can be used for the estimation of the rotor currents. The estimated rotor current on the stator reference frame can be given as follows:

$$\begin{bmatrix}\hat{i}_{\alpha r}^s\\ \hat{i}_{\beta r}^s\end{bmatrix} = \begin{bmatrix}\dfrac{\psi_{\alpha s} - L_s i_{\alpha s}}{M}\\ \dfrac{\psi_{\alpha s} - L_s i_{\alpha s}}{M}\end{bmatrix}. \quad (7)$$

The estimated rotor current given by (7) and transformed to the rotor reference frame using the transformation defined in (6) can be compared with the actual, measured rotor current. The external product of these two vector quantities gives the error for a hysteresis comparator, as shown in Fig. 2(a), which is

$$\varepsilon_r = \hat{i}_{\alpha r} i_{\beta r} - i_{\alpha r}\hat{i}_{\beta r}. \quad (8)$$

The error ε_r is the input of a hysteresis comparator that switches on or off when it is bigger than a certain *delta*. In [16], a study of the system with different values of *delta* was presented and shows that different values for *delta* give rise to different responses. It was concluded that the best value is *delta* = 0. The higher switching frequency of the hysteresis controller with *delta* = 0 does not give rise to chattering problems because it is limited to the sampling frequency used, and this

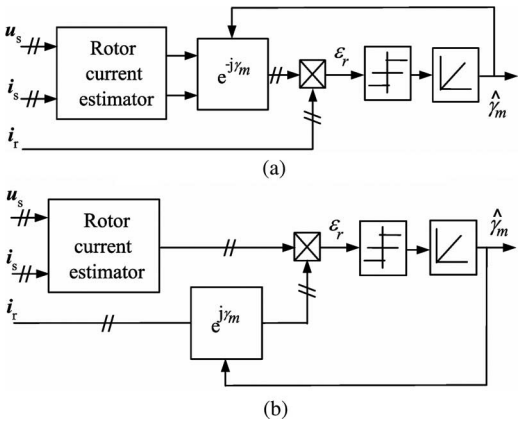

Fig. 2. Rotor-position-estimator structure. (a) Rotor-reference-frame implementation. (b) Stator-reference-frame implementation.

does not give rise to any power electronics commutation. The behavior of the hysteresis controller only results in adjustments of phase in software. The output of the hysteresis comparator will switch from two determined values and will be integrated leading to the estimated position γ_m, as shown in Fig. 2 where the exponential block represents the reference-frame transformation (6).

Because the output of the integrator is the estimated rotor position, the input will be the speed, i.e., the output of the hysteresis comparator is, in average and in steady state, the speed of the machine. Therefore, the output values of the hysteresis controller are the theoretical limits of the speed range of the estimator. Because the speed range of the DFIG is usually set on [0.7, 1.3] *p.u.*, in order to establish the appropriate speed range of the observer, the output of the hysteresis comparator was set in [0, 2] *p.u.*

Equation 8 can also be written in the form

$$\varepsilon_r = |\hat{i}_r \times i_r| = \hat{i}_{\alpha r} i_{\beta r} - i_{\alpha r} \hat{i}_{\beta r} = |\hat{\boldsymbol{i}}_r|.|\boldsymbol{i}_r|.\sin(\gamma_{\text{error}}). \quad (9)$$

The angle γ_{error} is defined between the vectors that represent the real and the estimated rotor currents. The hysteresis comparator adjusts the position of the rotor in response to this error. In steady state, the two vectors $\hat{\boldsymbol{i}}_r$ and $\boldsymbol{i}_r$ are moving at the same speed. If, in a considered instant of time, the estimated vector $\hat{\boldsymbol{i}}_r$ lags the measured vector current $\boldsymbol{i}_r$, the hysteresis comparator gives a positive output speed leading to an increase of the position and so the error will become smaller in the next sampling period. If $\hat{\boldsymbol{i}}_r$ leads $\boldsymbol{i}_r$, the output of the hysteresis controller will be zero giving a fixed position of the vector $\hat{\boldsymbol{i}}_r$, i.e., the vector $\hat{\boldsymbol{i}}_r$ will wait for $\boldsymbol{i}_r$. If γ_{error} is zero, the estimated rotor position coincides with the mechanical position of the rotor. The accuracy of the method depends on the accuracy of the rotor-currents measurement and on the accuracy of the estimation of the rotor currents. These depend on the stator-flux estimation and on the accuracy of the parameters of the machine (7). When a hysteresis controller is used with *delta* $= 0$, the critical parameter is the phase and not the amplitude of $\hat{\boldsymbol{i}}_r$ and $\boldsymbol{i}_r$.

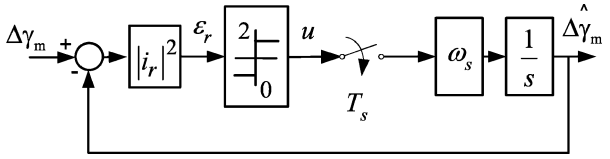

Fig. 3. Small-signal model for stability study.

The aforementioned method is implemented in the rotor reference frame because the phase comparison is performed using the original rotor current and the estimated rotor current is transformed to the rotor reference frame using the estimated rotor-position angle.The same principle can be used in the stator reference frame by transforming the measured rotor currents to the stator reference frame and comparing it with the estimated rotor current obtained by (7), [see Fig. 2(b)]. The method works well in these two reference frames as will be shown with experimental results. The stator-reference-frame implementation, which was adopted with the majority of the results presented in this paper, has the advantage of using variables with the same frequency independent of the speed, normally a higher frequency.

The detecting procedure of this method is very similar to the detecting flux method proposed in [6]. It is also similar to the method called rotor-current model reference adaptive system (MRAS) proposed in [8] and [10]. In [14] and [15], a rotor-position PLL method similar to the stator-reference-frame implementation is presented. The major advantages of the approach proposed in this paper are as follows.

1) It is not necessary to adjust any PI parameter;
2) It can be implemented on the stator or on the rotor reference frame.

III. Stability Analysis

The stability analysis can be performed using a small-signal model as in [8]. Linearizing (9) and considering that in steady state $|i_r| = |\hat{i}_r|$ results in

$$\varepsilon_r = |i_r|^2(\Delta\gamma_m - \Delta\hat{\gamma}_m). \quad (10)$$

The small-signal model for stability analysis, as shown in Fig. 3, can be obtained using (10) and Fig. 2. The natural sampling of the system is represented by the sample and hold element, as shown in Fig. 3.

According to the stability condition of sliding-mode systems, the stability is guaranteed if the product of the error ε_r by its derivative is always negative [19]. The fulfillment of this inequality ensures the convergence of the system state trajectories to the sliding surface $\varepsilon_r = 0$.

From the model, the following can be concluded using *p.u.* values:

$$\begin{aligned} \Delta\gamma_m &= \omega_s T_s \omega_m \\ \frac{d\varepsilon_r}{dt} &= |i_r|^2(\omega_s\omega_m - \omega_s u). \end{aligned} \quad (11)$$

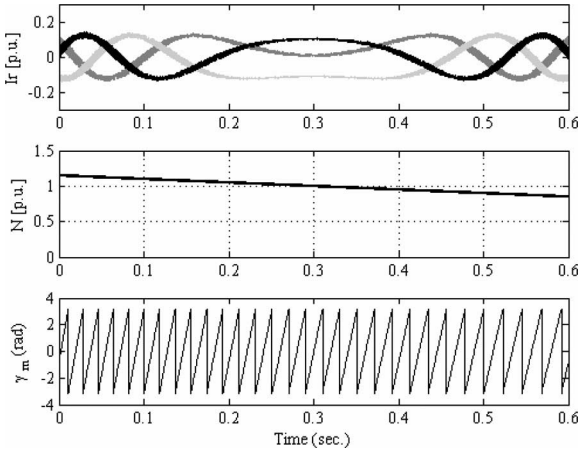

Fig. 4. Waveforms with small rotor currents ($I_{qr} = 0$, $I_{dr} = 0.15$ p.u.)

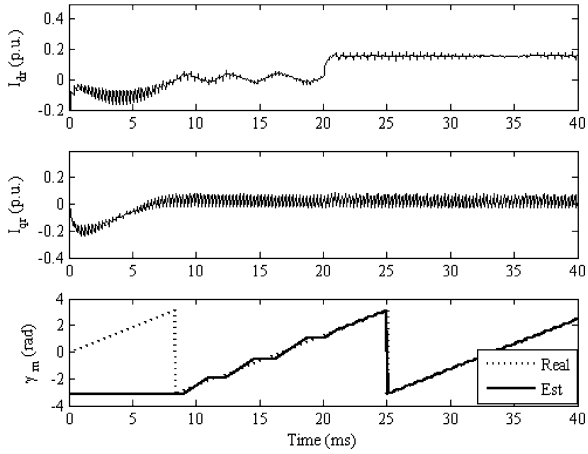

Fig. 5. Starting on the fly.

Analyzing the two possible conditions and considering the usual speed range ($0.7 < \omega_m < 1.3$), we have

$$\varepsilon_r < 0 \quad \rightarrow \quad u = 0 \rightarrow \frac{d\varepsilon_r}{dt} = |i_r|^2 \omega_s \omega_m > 0$$
$$\varepsilon_r > 0 \quad \rightarrow \quad u = 2 \rightarrow \frac{d\varepsilon_r}{dt} = |i_r|^2 \omega_s (\omega_m - 2) < 0. \quad (12)$$

This verifies the aforementioned stability condition.

IV. Simulation Results

A MATLAB/Simulink routine was constructed to determine the behavior of the proposed estimator included in the DFIG. The simulation results were obtained with the parameters of a 2-MW machine [18]. No problems of stability were verified.

The performance of the hysteresis comparator depends on the *delta* parameter [16]. After careful analysis of several simulation results, it was concluded that the best value is *delta* $= 0$. This nil value was adopted on the experimental apparatus.

It was also verified that the performance of this system is dependent on the rotor currents amplitude. Because the system is based on the comparison of rotor currents, when the load is small, the performance of the system is degraded. A value of 15% of rotor current was found in simulations as a limit for acceptable response.

The system has good responses in the speed range of the DFIG including the synchronous speed, as shown in Fig. 4. This figure shows the waveforms of the rotor currents when low level of rotor currents is considered (15%).

A simulation result showing a starting on the fly is presented in Fig. 5. On beginning, the rotor reference currents are nil and the system is not able to control the currents, as shown in the figure, and also it is not able to estimate the position. Near the instant $t = 10$ ms, the system starts to estimate the position, and when a step of the direct current reference occurs, the estimated position converges to the correct position.

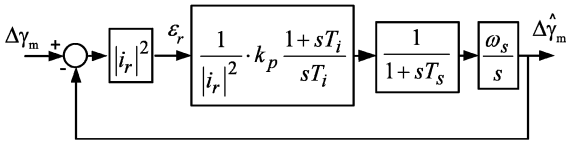

Fig. 6. Block diagram for the synthesis of the PI controller.

V. Synthesis of the PLL Method

In order to obtain a fair comparison between the PLL method and the method proposed here, a synthesis of the PI parameters is presented in this section.

The variable gain of the open-loop transfer function that depends on the squared rotor current is compensated on the PI parameters, as shown in Fig. 6, where the hysteresis controller of Fig. 3 was replaced by a PI controller. The sampling delay of the sample and hold element is now represented by the first-order block diagram with T_s time constant.

The determination of the PI controller parameters is a standard control problem similar to the speed-control loop of an electrical machine with inner torque control. The method generally used is the symmetrical optimum [20], [21]. According to this method, the k_p and T_i parameters are selected such that the amplitude and phase plot of the open-loop transfer function, as shown in Fig. 6, are symmetrical about the crossover frequency ω_c, which is the geometric mean of the corner frequencies $(1/T_s)$ and $(1/T_i)$ of the open-loop transfer function. Given a normalized factor α, the following can be obtained [20], [21]:

$$\omega_c = \frac{1}{\alpha T_s}$$
$$T_i = \alpha^2 T_s$$
$$k_p = \frac{1}{\alpha T_s \omega_s}. \quad (13)$$

Since T_s is determined by the sampling frequency used, the response of the system can be adjusted using the α parameter according to a required bandwidth. It is also necessary to consider

a damping factor ξ that is given by [21]

$$\xi = \frac{\alpha - 1}{2}. \tag{14}$$

By changing the α, the system damping or bandwidth can be adjusted as required.

VI. Experimental Results

This section presents some experimental results obtained in a prototype constructed for this purpose using a 3.2-kW wound induction machine. The estimation and control algorithms are implemented in a Microchip dsPIC30F4011. Two *dq* PI current controllers were implemented in a classical way. To obtain experimental results in real time, four PWM output channels with simple *RC* filters were used. The actual rotor position was measured using an incremental encoder and the quadrature encoder interface (QEI) of another dsPIC30F4011. On the oscilloscope, the actual measured and the estimated rotor positions can be compared.

The PLL system described in [14] and [15] was also implemented. The PI parameters were fixed in order to get a bandwidth of 200 Hz. The sampling frequency adopted was 10 kHz.

A. Practical Issues

In practice, it is necessary to eliminate the effect of initial conditions when the estimator defined by (2) is used. The simplest solution consists in using a low-pass filter replacing the pure integrator. This is achieved introducing a feedback loop leading to

$$\psi_{\alpha s} = \omega_s \int (u_{\alpha s} - r_s i_{\alpha s} - k_f \psi_{\alpha s}) dt$$
$$\psi_{\beta s} = \omega_s \int (u_{\beta s} - r_s i_{\beta s} - k_f \psi_{\beta s}) dt. \tag{15}$$

The elimination of these effects is dependent of the k_f parameter. However, this technique produces an error of amplitude and phase. This can be analyzed using the transfer function of the low-pass filter, which is

$$\frac{\psi(s)}{(u - ri)(s)} = \frac{1}{(j\omega/\omega_s) + k_f}. \tag{16}$$

Because the flux estimator is working always at the mains frequency $\omega = \omega_s$, the error in amplitude and the error in phase can be determined by

$$|G_{\text{error}}| = \frac{1}{\sqrt{1 + k_f^2}}$$
$$\text{Phase}_{\text{error}} = \theta = atn(k_f). \tag{17}$$

For stator-flux orientation, the quantity of interest is the phase angle of the stator flux. Because γ_s obtained with (3) has the error estimated with (17), the corrected stator-flux position is given by $\gamma_s - \theta$. A better angle can be obtained easily using well-known trigonometric formulas. Since k_f is a small number,

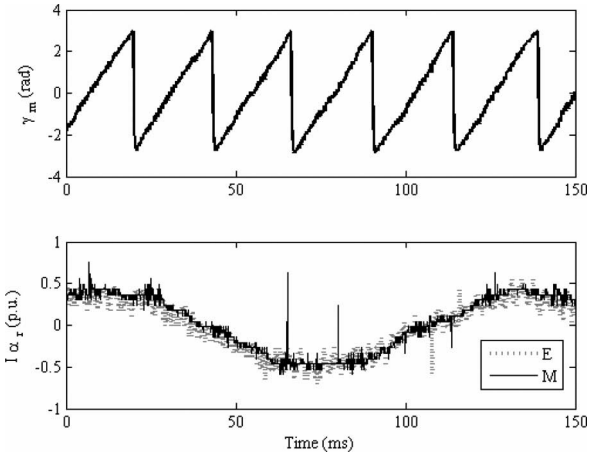

Fig. 7. Implementation on the rotor reference frame.

this leads to

$$\cos\theta \cong 1 \quad \sin\theta \cong k_f$$
$$\cos(\gamma_s - \theta) = \cos\gamma_s + k_f \sin\gamma_s$$
$$\sin(\gamma_s - \theta) = \sin\gamma_s - k_f \cos\gamma_s. \tag{18}$$

The correction given by (18) can be easily implemented giving rise to significant benefits.

B. Experimental Results in Steady State

The results are presented using *per unit* values defined with the peak of the rated values. All these figures were obtained with the *dq* rotor current control.

Fig. 7, obtained with the hysteresis controller implemented on the rotor reference frame, shows the estimated position γ_m, the rotor current, and the estimated rotor current on the rotor reference frame.

The rotor current and its estimated value are in phase. This shows the correctness of the method.

A similar result, obtained with the estimation algorithm working on the stator reference frame, is presented in Fig. 8(a), where the measured position obtained with the encoder is also present. In this case, the estimated and measured rotor currents are indistinguishable from one another (on the stator reference frame). Very similar results, obtained using the PLL method, are presented in Fig. 8(b).

It was verified that the starting on the fly is as expected and so there is no need of any care with the initial conditions. This starting transient occurs more easily when the hysteresis comparator is used. The safe operation down to 15% was also verified experimentally in the hysteresis controller.

C. Experimental Results With Steps on the Reference Currents

The objective of this section is to show that the system is appropriate for the implementation of stator-flux orientation.

This is the major purpose of the rotor-position-estimation system. In this case, it can be shown that the rotor quadrature current acts on the active power and the direct current acts on

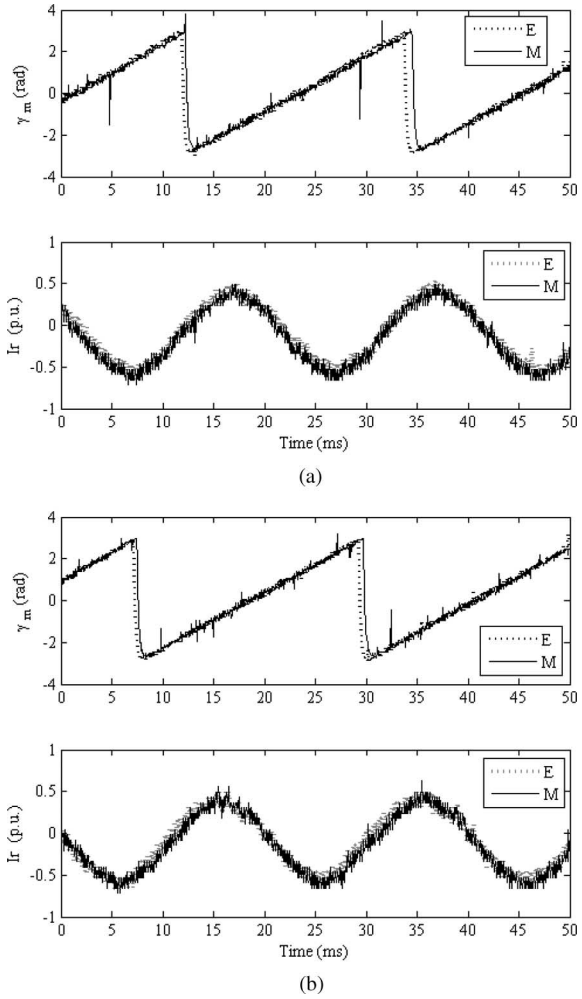

Fig. 8. Implementation on the stator reference frame. (a) Using a hysteresis controller. (b) Using the PLL method.

the reactive power. These relations are given by

$$P_s = r_s\left(i_{ds}^2 + i_{qs}^2\right) + \frac{M^2}{L_s}\psi_s i_{qr}$$
$$Q_s = \omega_{s(pu)}\psi_s\left(\frac{\psi_s}{L_s} - \frac{M}{L_s}i_{dr}\right). \tag{19}$$

Equation (19) shows that, if the rotor quadrature current is constant, the power transferred to the rotor, $P_e = P_s - p_{Js}$ remains also constant. Conversely, if the rotor direct current remains constant, the stator reactive power also remains constant.

The results obtained are presented in Figs. 9–11. These figures show that the decoupling of the active and reactive power can be partially achieved.

In Fig. 9(a), step of 80% on the rotor-reference direct current was applied. The quadrature current was maintained constant in a small value (15%). At the beginning, when the current is small, the system estimates the position with a visible error. This error decreases rapidly when the current increases. It can be verified that P_e is almost constant.

Similar results for the PLL system are also presented. It can be concluded that the differences are small. However, these results

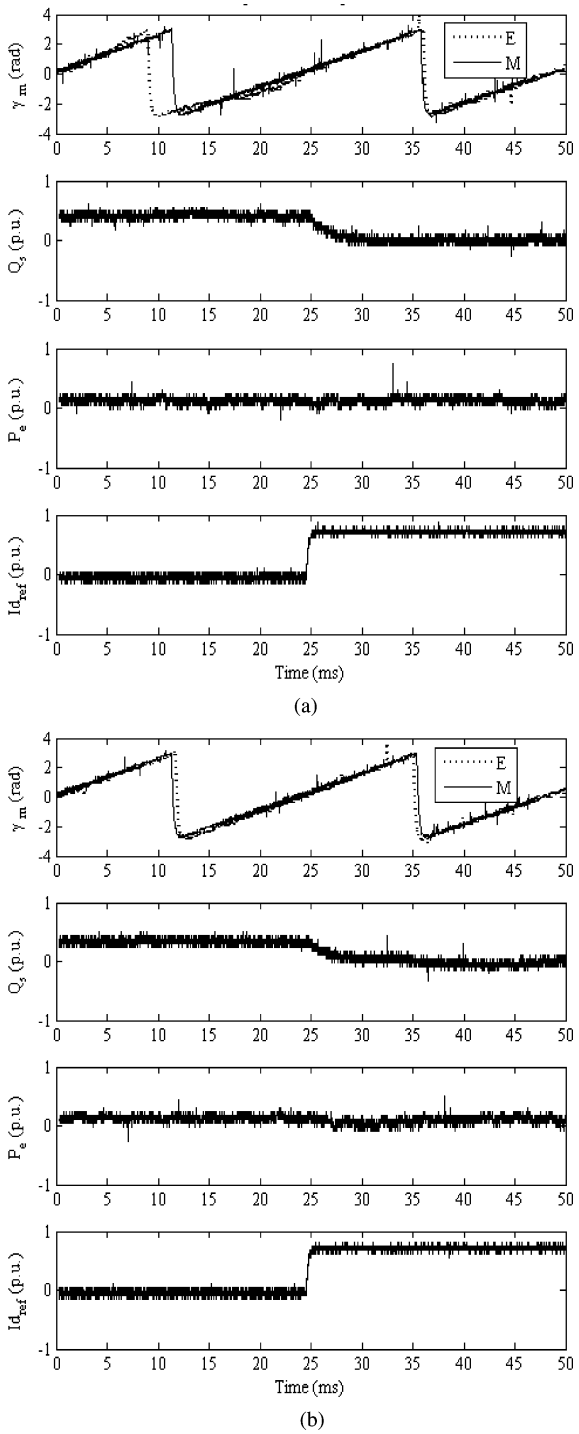

Fig. 9. Step response to rotor direct current. (a) Response with a hysteresis controller. (b) Response of the system based on a PLL.

were not obtained exactly in the same situation because the rotor current is a little bit higher.

The response to a step of 80% on the rotor quadrature current is presented in Fig. 10(a). In this case, the rotor direct current was maintained in a constant value (15%). It can be observed that there is a small coupling in the stator reactive power. If the correcting system presented in (18) is not implemented, this coupling will be more visible.

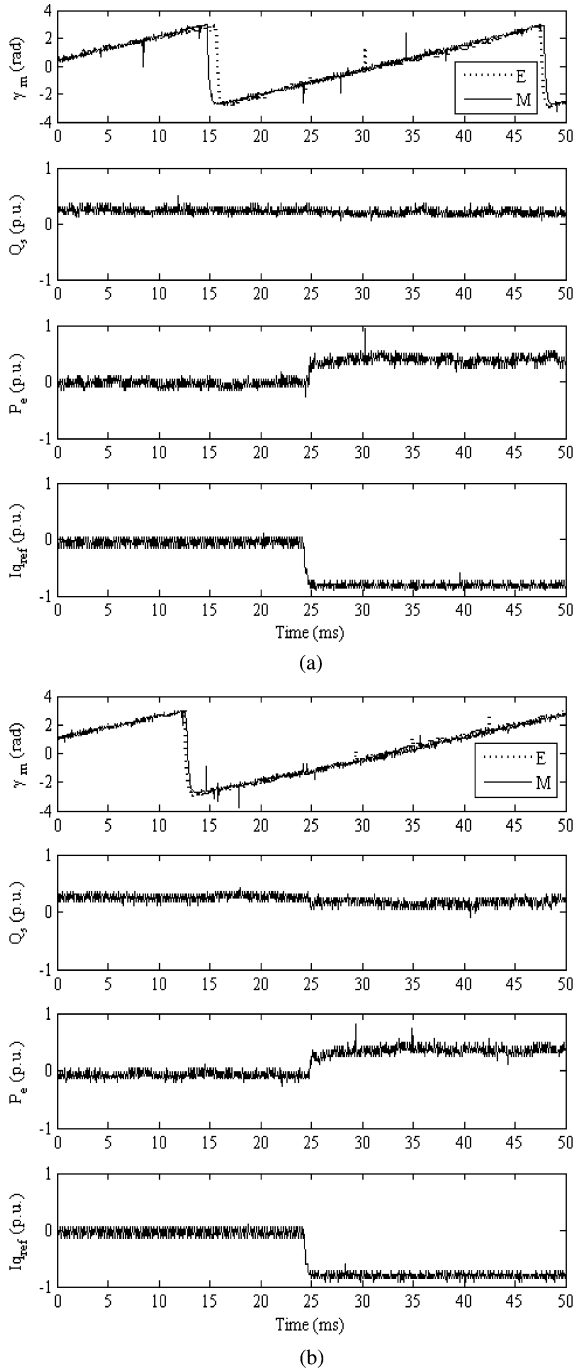

Fig. 10. Step response to rotor quadrature current. (a) Response with a hysteresis controller. (b) Response of the system based on a PLL.

A similar result for the PLL system is also obtained, as shown in Fig. 10(b), which is very similar to the hysteresis controller.

When a quadrature step current is applied, the DFIG produces a corresponding torque. If the load torque is small, the system starts to accelerate and will cross the synchronous speed, as shown in Fig. 11. Note that the amplitude of the rotor currents remains constant and the slip frequency decreases to zero and increases again.

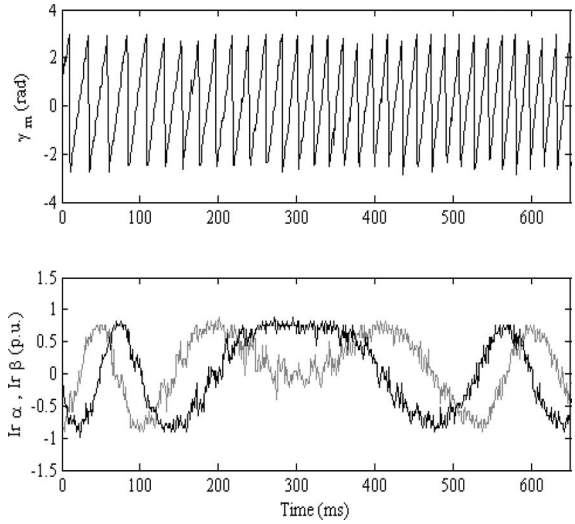

Fig. 11. Crossing the synchronous speed.

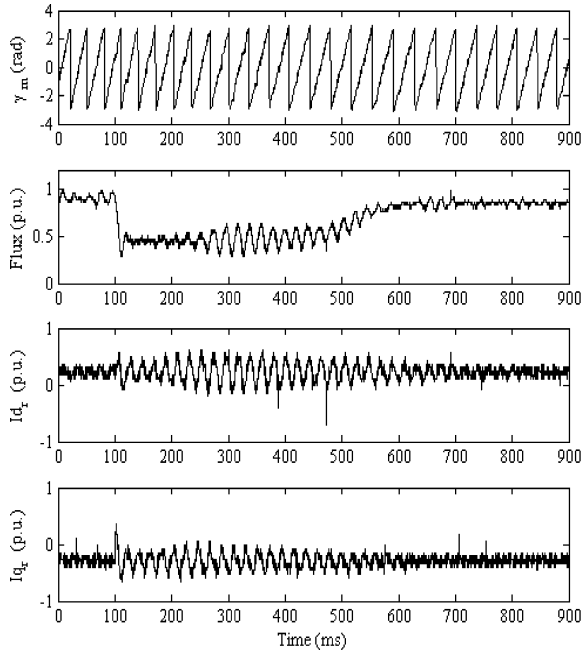

Fig. 12. Responses to a voltage dip of 50% amplitude using a hysteresis controller.

D. Results During a Voltage Dip

The behavior of the system proposed in this paper during voltage dips is presented in Figs. 12 and 13. The amplitude of the voltage dip is approximately 50%. The figure shows the behavior of the estimated position, the amplitude of the flux vector, and the direct and quadrature rotor currents. It can be seen that the system presents good results during this transient. The oscillations presented are due to the natural frequencies of the system.

Fig. 13 shows thesame response for two cases when a PLL system is used. In the first case (100-Hz bandwidth), three

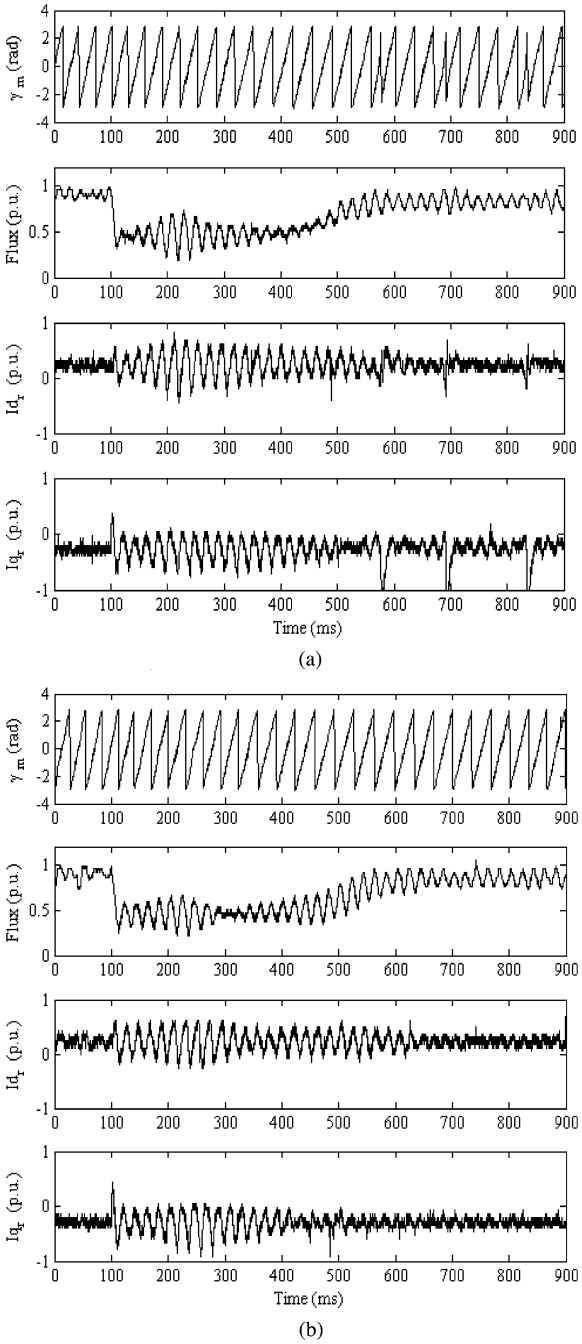

Fig. 13. Responses to a voltage dip of 50% amplitude using a PLL system. (a) Using a PLL with 100-Hz bandwidth. (b) Using a PLL with 200-Hz bandwidth.

failures can be seen near the time instants 600, 700, and 850 ms. These failures produced considerable torque variations and were found during the experiments when an insufficient bandwidth was used in the synthesis of the PLL. This shows that the synthesis of the PI controller is critical. The problem was solved increasing the bandwidth to 200 Hz, as shown in Fig. 13(b). It was also verified that both the rotor current necessary for synchronization and the time of synchronization increase when a lower bandwidth is used. The failures shown in Fig. 13(a) never occurred with the hysteresis controller.

VII. Conclusion

The paper presents a sensorless system for the estimation of the rotor position of the DFIG. The proposed sensorless algorithm fulfills the requirements of this system in the general applications when a restricted speed range is necessary. The operation at synchronous speed, corresponding to zero rotor frequency is stable and presents no special problem. The starting on the fly of the system is established easily.

Although the performance of the system is dependent on the rotor current, it was shown that the system works acceptably well with low currents as low as 15% of rotor current.

Stator and rotor reference frame implementation can be easily achieved.

Experimental results showing the system working in different situations are presented. When compared with the PLL system, tuned to have a bandwidth as high as 200 Hz, this method presents similar dynamic behavior.

Appendix

Parameters of the DFIG

Induction machine: stator 380 V, 8.1 A, rotor 110 V, 19 A, 3.2 kW, four poles, 1400 r/min, $L_s = 1.62$ p.u., $M = 1.17$ p.u., $r_s = 0.06$ p.u.

References

[1] R. Pena, J. C. Clare, and G. M. Asher, "Doubly fed induction generator using back-to-back PWM converters and its application to variable-speed wind-energy generation," *IEE Proc. Elect. Power Appl.*, vol. 143, no. 3, pp. 231–241, May 1996.

[2] E. Bogalecka, "Power control of a double fed induction generator without speed or position sensor," in *Conf. Rec. 1993 Eur. Power Electron. Appl. (EPE)*, pt. 8, vol. 377, ch. 50, pp. 224–228.

[3] E. Bogalecka and Z. Krzeminski, "Sensorless control of double fed machine for wind power generators," presented at the Eur. Power Electron. Appl.-Electronics and Motion Control (EPE-PEMC) Conf., Dubrovnik-Cavat, Croatia, 2002.

[4] Z. Krzeminski, A. Popenda, M. Melcer, and P. Ladach, "Sensorless control system of double fed induction machine with predictive current controller," presented at the Eur. Power Electron. Appl. (EPE) 2001 Conf., Graz, Austria.

[5] R. Datta and V. T. Rangaanathan, "A simple position-sensorless algorithm for rotor-side field-oriented control of wound-rotor induction machine," *IEEE Trans. Ind. Electron.*, vol. 48, no. 4, pp. 786–793, Aug. 2001.

[6] W. Zimmermann, "High-dynamic AC machine control without speed or position sensor," *Eur. Trans. on Elect. Power (ETEP)*, vol. 6, no. 1, pp. 47–51, Jan./Feb. 1996.

[7] R. Cárdenas, R. Peña, G. Asher, J. Clare, and J. Cartes, "MRAS observer for doubly fed induction machines," *IEEE Trans. Energy Convers.*, vol. 19, no. 2, pp. 467–468, Jun. 2004.

[8] R. Cárdenas, R. Peña, J. Proboste, G. Asher, and J. Clare, "Rotor current based MRAS observer for doubly-fed induction machines," *Electron. Lett.*, vol. 40, no. 12, pp. 769–770, Jun. 2004.

[9] R. Cárdenas, R. Peña, J. Proboste, G. Asher, and J. Clare, "Sensorless control of a doubly- fed induction generator for stand alone operation," in *Proc. 35th Annu. IEEE Power Electron. Spec. Conf.*, Aachen, Germany, 2004, pp. 3378–3383.

[10] R. Peña, R. Cárdenas, J. Proboste, G. Asher, and J. Clare, "Sensorless control of doubly-fed induction generators using a rotor-current-based MRAS observer," *IEEE Trans. Ind. Electron.*, vol. 55, no. 1, pp. 330–339, Jan. 2008.

[11] L. Morel, H. Godfroid, A. Mirzaian, and J. M. Kaufmann, "Double-fed induction machine: Converter optimization and field oriented control without position sensor," in *Proc. Inst. Elect. Eng. (IEE) Electr. Power Appl*, vol. 145, no. 4, pp. 360–368, Jul. 1998.

[12] L. Xu and W. Cheng, "Torque and reactive power control of a doubly fed induction machine by position sensorless scheme," *IEEE Trans. Ind. Appl.*, vol. 31, no. 3, pp. 363–642, May/Jun. 1995.
[13] B. Hopfensperger, D. J. Atkinson, and R. A. Lakin, "Stator-flux-oriented control of a doubly-fed induction machine with and without position encoder," *Proc. Inst. Elect. Eng. (IEE) Electr. Power Appl*, vol. 147, no. 4, pp. 241–250, Jul. 2000.
[14] B. Shen, B. Mwinywiwa, Y. Zhang, and B.-T. Ooi, "Sensorless maximum power point tracking of wind by DFIG using rotor position phase lock loop (PLL)," *IEEE Trans. Power Electron.*, vol. 24, no. 24, pp. 942–951, Apr. 2009.
[15] B. Mwinyiwiwa, Y. Zhang, B. Shen, and B.-T. Ooi, "Rotor position phase-locked loop for decoupled P-Q control of DFIG for wind power generation," *IEEE Trans. Energy Convers.*, vol. 24, no. 3, pp. 758–765, Sep. 2009.
[16] G. D. Marques, V. Fernão Pires, S. Sousa, and D. M. Sousa, "Evaluation of a DFIG rotor position-sensorless detector based on a hysteresis controller," presented at the Power Eng. Conf., Costa da Caparica, Lisbon, 2009.
[17] D. G. Forchetti, G. O. Garcia, and M. Inés Valla, "Adaptative observer for sensorless control of stand-alone doubly fed induction generator," *IEEE Trans. Ind. Electron.*, vol. 56, no. 10, pp. 4174–4180, Oct. 2009.
[18] A. Petersson, T. Thiringer, L. Harnefors, and T. Petru, "Modeling and experimental verification of grid interaction of a DFIG wind turbine," *IEEE Trans. Energy Convers.*, vol. 20, no. 4, pp. 878–886, Dec. 2005.
[19] F. A. Silva and S. Pinto, "Control methods for switching power converters," in *Power Electronics Handbook*, M. H. Rashid, Ed., 2nd ed. Academic Press, Elsevier, ch. 34, pp. 935–998.
[20] V. Kaura and V. Blasko, "Operation of a phase locked loop system under distorted utility conditions," *IEEE Trans. Ind. Appl.*, vol. 33, no. 1, pp. 58–63, Jan./Feb. 1997.
[21] W. Leonard, *Control of Electrical Drives*. Berlin, Germany: Springer-Verlag, 1990.

G. D. Marques (M'95) was born in Benedita, Portugal, on March 24, 1958. He received the Dipl. Ing. and Ph.D. degrees in electrical engineering from the Technical University of Lisbon, Lisbon, Portugal in 1981 and 1988, respectively.

Since 1981, he has been with the IST, Technical University of Lisbon, where he teaches Power Systems in the Department of Electrical and Computer Engineering. He is also a Researcher at the Center for Innovation in Electrical and Energy Engineering. His research interests include electrical machines, static power conversion, variable-speed drive and generator systems, and harmonic compensation systems and distribution systems. He is an Associate Professor since 2000.

V. Fernão Pires (M'96–SM'09) received the B.S. degree in electrical engineering from the Institute Superior of Engineering of Lisbon, Lisbon, Portugal, in 1988, and the M.S. and Ph.D. degrees in electrical and computer engineering from the Technical University of Lisbon, Lisbon, in 1995 and 2000, respectively.

Since 1991, he has been a member of the teaching staff at the Department of Electrical Engineering, Superior Technical School of Setúbal, Polytechnic Institute of Setúbal, Portugal, where he is currently a Professor, teaching power electronics and control of power converters. He is also a Researcher at the Center for Innovation in Electrical and Energy Engineering. His current research interests include the areas of topologies and control of power converters.

Sérgio Sousa was born in Almada, Portugal, on September, 10, 1971. He received the B.S. degree in electrical engineering from the Superior Institute of Engineering of Lisbon, Polytechnic Institute of Lisbon, Lisbon, Portugal, in 1995, and the Dipl. Ing. and M.S. degrees in electrical and computer engineering from the Superior Technical School of Setúbal, Polytechnic Institute of Setúbal, Setúbal, Portugal, in 2007 and 2009, respectively.

Since 2009, he has been a member of the teaching staff at the Department of Electrical Engineering, Superior Technical School of Setúbal, Polytechnic Institute of Setúbal, Setúbal, Portugal. His research interests include power electronics, and digital control of electrical drives and machines.

Duarte M. Sousa (M'09) was born in Viana do Castelo, Portugal, in 1970. He received the Dipl. Ing., M.S., and Ph.D. degrees in electrical and computer engineering from the Instituto Superior Técnico and the Technical University of Lisbon, Lisbon, Portugal, in 1993, 1996, and 2003, respectively.

In 1993 he joined the Technical University of Lisbon, Lisbon, where he has been an Assistant Professor since 2003.